Available online at www.sciencedirect.com

ScienceDirect

Procedia Structural Integrity 39 (2022) 194–203

Structural Integrity Procedia

www.elsevier.com/locate/procedia

7th International Conference on Crack Paths

Three-dimensional fatigue crack propagation by means of first order SIF approximation

Paolo Livieri[a, *], Fausto Segala[b]

[a]*Dept of Engineering, University of Ferrara, via Saragat 1, 44122, Ferrara, Italy*
[b]*Dept of Mathematics, University of Ferrara, via Saragat 1, 44122, Ferrara, Italy*

Abstract

In this paper we make use of a closed-form solution for mode I Stress Intensity Factors (SIF) in three-dimensional planar flaws based on homotopy transformations of a disc. The utilised equations are very accurate when the flaw is a small deviation from a circle. Under the hypothesis of an isolated crack, the SIF at each point of the crack border is calculated to assess the crack shape after propagation. The solution is proposed in terms of the Fourier series and the crack growth rate equation is taken according to Paris' low. Many examples are proposed with the aim of predicting the final shape of different types of embedded planar flaws in butt welded joints under fatigue tensile loading.

Keywords: Stress intensity factor; Fatigue propagation; Welded joints

1. Introduction

The Stress Intensity Factor (SIF) of two-dimensional cracks can be obtained without particular problems by means of fracture mechanics textbooks [1, 2] or by applying formulas present in the scientific literature. However, in the case of three-dimensional planar cracks, the equation for SIF calculation is not so manageable and is often overcome by

* Corresponding author.
E-mail address: paolo.livieri@unife.it

10.1016/j.prostr.2022.03.088

using numerical applications. In fact, apart from some particular geometrical cases, such as elliptical cracks [3, 4], there is no exact analytical solution for generic crack shape contours in the literature.

Nomenclature

a	radius of reference circle
K_I	mode I stress intensity factor
ΔK	range of K_I
K_{th}	threshold for stress intensity factor
x,y	actual cartesian reference system
$\bar{x}, \bar{y}$	actual cartesian reference system
s	arch-length
$\bar{\rho}$	actual radius
ρ	non-dimensional radius
$\Delta\sigma_n$	range of nominal stress

In order to avoid this problem, Oore-Burns [5] introduced a three-dimensional weight function which gives an exact solution in the case of a circular or tunnel crack. However, when an elliptical crack is assumed, the authors have shown that, under remote uniform tensile loading, the Oore-Burns integral gives a first order approximation of the SIF along the whole crack front and a second order approximation is also possible [6]. Furthermore, the first order equation is very close to the first order approximation of Irwin's [4] exact solution.
The SIF calculation around the crack contour is more complicated if the propagation phase is considered because even if the initial crack is assumed elliptical after the growth, the shape is not elliptical. In order to overcome this problem, an elliptical shape is often maintained. For instance, in reference [7], an elliptical-arc surface flaw is always assumed to exist in notched round bars under cyclic tension and bending, for different values of stress concentration factors. So that, after the first crack shape assumption, the subsequent crack growth phase under cyclic loading was examined through a numerical procedure which takes into account the computed SIF values by considering a crack front as an elliptical arc. This hypothesis is also considered to estimate the fatigue life of welded joints where the shape of a semi-elliptical crack is usually kept [8, 9, 10,[11]].
In order to overcome the exact stress intensity factors of a generical crack, Murakami and Endo [12] proposed the $\sqrt{area}$ as an empirical parameter for the evaluation of the fatigue limit linked to the maximum stress intensity factors under mode I loadings ($K_{I,max}$) of small convex cracks. On the basis of several examples of flaw shapes, Murakami and Nemat-Nasser [13] proposed the simple formula $K_{I,max} = Y \sigma \sqrt{\pi \sqrt{area}}$, where Y is a coefficient which is evaluated as best fitting the numerical and analytical results (Y=0.63 for a surface crack). However, in light of the first order approximation of the crack border, in reference [14],an approximated analytical model of the first order was proposed for the SIF calculation based on the Oore-Burns integral. So that, an explicit analytical equation for SIF calculations could be useful for estimating the SIF of internal irregular small defects or irregular cracks. Furthermore, when the flaw can be considered as a star domain, the full Oore-Burns solution can be used [15,16].

The aim of this paper is to propose a numerical model for fatigue crack propagation based on the first order approximation of the SIF along the whole crack front. More precisely, for small embedded cracks in butt welded joints, we are able to compute the SIF in closed form and then consider the propagation phase of the defects. The material is considered as linear elastic while the propagation regime is considered according to the Paris-Erdogan equation. Some examples will be proposed and the final shape of the crack will be discussed.

2. Stress intensity factor evaluation

2.1. Oore-Burns integral

The mode I loading stress intensity factor of a planar crack Ω in a three-dimensional body can be estimated by means of the Oore-Burns weight function [5]. When the crack takes a special configuration such as a disc or a tunnel crack, this weight function gives the exact solution. Let Ω be an open bounded, simply connected, bounded open subset of the plane. We set:

$$f(Q) = \int_{\partial\Omega} \frac{ds}{|Q-P(s)|^2}, \qquad Q \in \Omega \tag{1}$$

where $Q \in \Omega$, s is the arc-length on $\partial\Omega$ and P(s) describes $\partial\Omega$. Then the O-integral is defined as:

$$K_I(Q') = \frac{\sqrt{2}}{\pi} \int_{\Omega} \frac{\sigma_n(Q)\,h(Q)}{|Q-Q'|^2} d\Omega \;, \qquad Q' \in \partial\Omega \tag{2}$$

where σ_n(Q) is the nominal stress over the Ω region evaluated without taking into account the crack and $Q \in \Omega$ with

$$h(Q) = \frac{1}{\sqrt{f(Q)}} \tag{3}$$

while $Q' \in \partial\Omega$. The nominal stress σ_n(Q) can be evaluated analytically or by means of FE analysis.
In this work, we assume a constant value for nominal stress σ_n, therefore we consider the case of small embedded defects. Figure 1 shows the reference scheme for a crack in an infinite body.

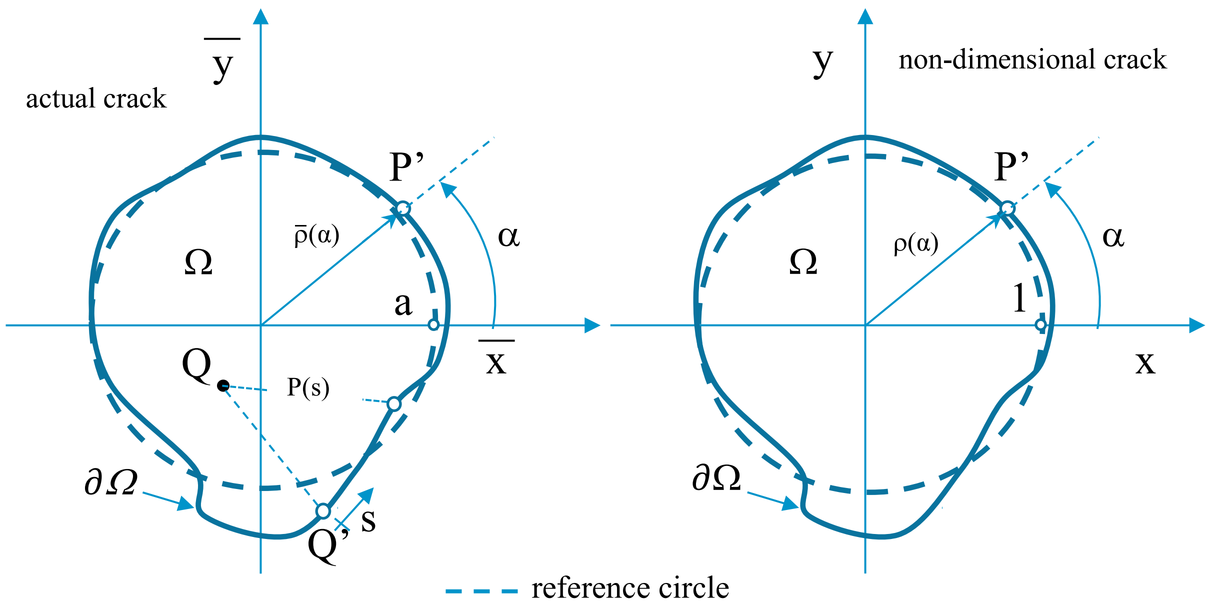

Fig. 1. Perturbation of the circular flaw with a=1.

2.2. Analytical equation for the SIF based on first order approximation

Let Ω be an open bounded simply-connected subset of the plane as reported in Fig. 1 with a=1 ($\rho(\alpha)=\bar{\rho}(\alpha)/a$). In a previous paper [17], we considered $\partial\Omega$ as a distortion of the unitary circle in terms of a continuous function R=R(ε, ψ) (homotopy) of class C^1 with respect to ψ, with the possible exception of a finite number of values (edges) and of

class C^2 with respect to ε, where $0\leq \varepsilon \leq 1$ is a parameter and $0\leq \psi \leq 2\pi$ is the angle.
By means of the Taylor expansion, we have

$$K_I(\varepsilon,\alpha) = \frac{2}{\sqrt{\pi}} + \varepsilon \frac{\partial K_I}{\partial \varepsilon}(0,\alpha) + O(\varepsilon^2) \tag{4}$$

(see reference [18] for the non-trivial detailed calculation of $\frac{\partial K_I}{\partial \varepsilon}(0,\alpha)$).
In reference [18] we obtained the following approximation for the Oore-Burns integral (1) as a function of the angle α:

$$K_I(\varepsilon,\alpha) = \frac{2}{\sqrt{\pi}} \left\{ 1 + \varepsilon \sum_{-\infty}^{+\infty} c_n E_n e^{in\alpha} \right\} + O(\varepsilon^2) \tag{5}$$

where c_n are the Fourier coefficients of the first order crack front position $\alpha \to S(\alpha) = \frac{\partial R}{\partial \varepsilon}(0,\alpha)$ in the sense that $S(\alpha) = \sum_{-\infty}^{+\infty} c_n e^{in\alpha}$.
The E_n coefficients are independent of the homotopy R and are reported in Table 1 (for the complete formulae of E_n coefficients see reference [18]).
In general, by considering that an *a*-dilatation of Ω under uniform normal tension σ_n produces factor $\sqrt{a}$ in the expression of K_I, from (5) we are able to state the following final equation:

$$K_I(\varepsilon,\alpha) = \frac{2\sigma_n\sqrt{a}}{\sqrt{\pi}} \left\{ 1 + \varepsilon \sum_{-\infty}^{+\infty} b_n E_n e^{in\alpha} \right\} + O(\varepsilon^2) \tag{6}$$

where b_n are the Fourier coefficients of $\alpha \to \frac{1}{a}\frac{\partial R}{\partial \varepsilon}(0,\alpha)$ and $R(\varepsilon,\alpha)$ describes the boundary of $\partial\Omega(\varepsilon)$.
Now let $\rho=\rho(\alpha)$ the polar equation of $\partial\Omega$ and consider the homotopy $R(\varepsilon,\alpha) = 1 + \varepsilon(\rho(\alpha) - 1)$. If Ω is a slight distortion of a disc of radius *a* under remote uniform tensile stress σ_n, by choosing $\varepsilon=1$, the SIF turns out to be:

$$K_I(\alpha) \approx \frac{2\sigma_n\sqrt{a}}{\sqrt{\pi}} \left\{ \frac{1+b_0}{2} + \sum_{|n|\geq 2} b_n E_n e^{in\alpha} \right\} \tag{7}$$

where, in this case, b_n are the Fourier coefficients of $\bar{\rho}(\alpha)$. Eq. (7) is the first order approximation of the Oore-Burns integral (2).
Finally, if we take into account the Fourier series in the form:

$$\rho(\alpha) = b_0 + \sum_{n=1}^{\infty} p_n \cos(n\alpha) + \sum_{n=1}^{\infty} q_n \sin(n\alpha) \tag{8}$$

with

$$b_0 = \frac{1}{2\pi}\int_0^{2\pi}\rho\, d\alpha; \qquad p_n = \frac{1}{\pi}\int_0^{2\pi}\rho\cos(n\alpha)\, d\alpha; \qquad q_n = \frac{1}{\pi}\int_0^{2\pi}\rho\sin(n\alpha)\, d\alpha; \qquad (9\ a,\ b,\ c)$$

the expression of K_I becomes:

$$K_I(\alpha) \approx \frac{2\sigma\sqrt{a}}{\sqrt{\pi}}\left\{\frac{1+b_0}{2} + \sum_{n\geq 2} E_n\left[p_n\cos(n\alpha) + q_n\sin(n\alpha)\right]\right\} \qquad (10)$$

The asymptotic behaviour of E_n and the hypothesis on R (and therefore on ρ) ensure the convergence of the series (10).

Table 1. E_n coefficients

n	E_n	n	E_n
0	½	6	-1.58042
1	0	7	-1.81911
2	-0.4	8	-2.04377
3	-0.74286	9	-2.2566
4	-1.04762	10	-2.45929
5	-1.32468	11	-2.65318

3. Propagation phase

By means of Eq. (10), the stress intensity factors on the whole crack contour can be easily calculated provided that the b_0, p_i and q_i coefficients are estimated. Now, in order to use Eq. (10) for the assessment of the propagation of an embedded crack, we consider a butt welded joint subjected to a fatigue loading with a nominal ratio equal to zero. The growth rate model is taken according to Paris' model [19]:

$$\frac{da}{dN} = C\ \Delta K^m \qquad (11)$$

If $\Delta K \leq \Delta K_{th}$, the crack growth ratio da/dN is set to zero. Obviously, more complicated propagation models could be used in the future that take into account the closure effect or short crack [20,21,22]. In the specific case of welded joints according to Hobbacher [23], we consider the reference values of Table 2 for steel joints.

In order to evaluate the final crack shape, as a first step, the stress intensity factors are calculated by means of Eq. (9) . In all analyses, we use half of the maximum diameter of the actual crack to obtain the non-dimensional radius ρ(α) in Eq. (9) (a=max diameter of crack / 2). Then, by using Eq. (11), the local crack growth *da(α)* is evaluated along the whole boundary and the new shape is carried out. The increment of *da(α)* is assumed according to the outward normal and the use of Eq. (8) simplifies the evaluation of the normal as a function of *α*.

Table 2. Parameters of Paris' power law and threshold data for steel [23]

Units	Paris' power law parameters	Threshold ΔK_{th} values
K_I [N mm$^{-3/2}$]	$C = 5.21 \cdot 10^{-13}$	170
da/dN [mm/cycle]	m=3	

As an example, Figure 2, shows a generis crack shape with a maximum diameter of about 0.44 mm subjected to a nominal stress range $\Delta\sigma_n$ of 350 MPa. After $5 \cdot 10^4$ cycles of propagation, the shape becomes close to a circular disc as reported in Figure 3. In order to measure the distortion of the crack with respect to the reference circle of radius *a*, we consider the *t* parameter defined as follows:

$$t = 1 + \sum_{i=1}^{N} \left|\frac{p_i}{b_0}\right| + \sum_{i=1}^{N} \left|\frac{q_i}{b_0}\right| \tag{12}$$

When *t* is equal to the unity the crack becomes a circle. The trend of *t* is reported in Figure 4. After an initial quick decreasing, the final value of *t* tends asymptotically to the unity. When the shape of the crack is not uniform, its growth depends on α. As the initial SIF in A is less than ΔK_{th}, the crack does not increase in the first stage of propagation as reported in Figure 5. On the contrary, the crack grows right from the beginning in B. The size trend of Figure 5 in points A and B confirms, in another way, the results of Figures 3 and 4.

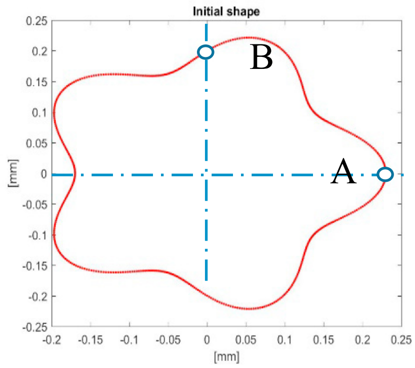

Fig.2. Initial size of the crack.

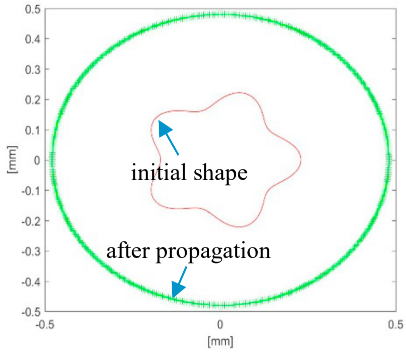

Fig. 3. Final shape and size after $5 \cdot 10^4$ cycles of propagation ($\Delta\sigma_n$=350MPa).

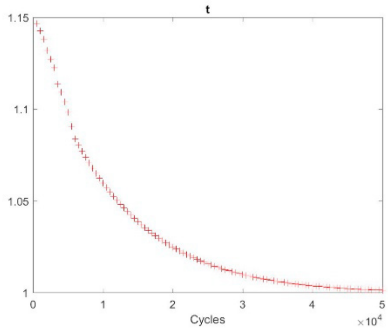

Fig. 4. Trend of the *t* parameter for the crack of Figure 2.

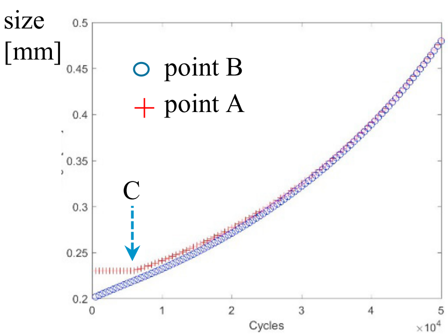

Fig. 5. Trend of size in points A and B of Figure 2

Finally, Table 3 shows some examples of crack growth under the uniform nominal stress range. The trend of *t* is very similar to the example shown in Figure 4. Independently from the initial shape, the crack quickly approaches a circular disc. It should be noted that in many experimental cases of axial fatigue loading, the fracture surface shows a circular area around an embedded critical flaw [24, 25, 26, 27, 28]. Similar results were also obtained by Lazarus [29] by means of Bower and Ortiz's finite perturbation method [30]. However, specific software is needed for the finite perturbation method. On the contrary, this paper requires only the implementation of Equation (8) to evaluate the shape of the crack, Equation (10) for evaluation of the SIF and Eq. (11) for the size increment.

Table 3. Examples of crack growth under the uniform nominal stress range

<table>
<tr><th>case</th><th>crack shape</th><th>t parameter</th></tr>
<tr><td>1</td><td>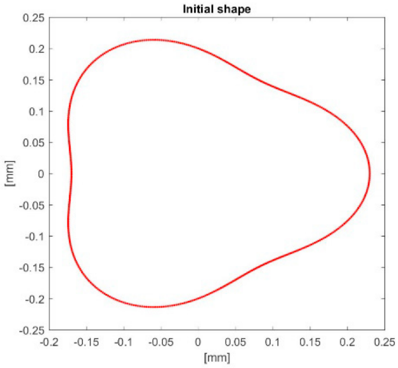
</td><td>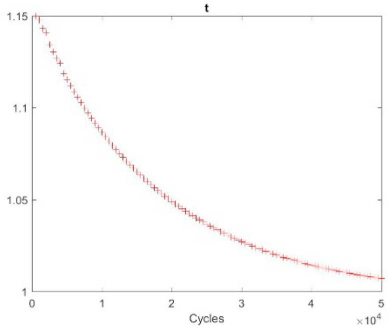
</td></tr>
<tr><td>2</td><td>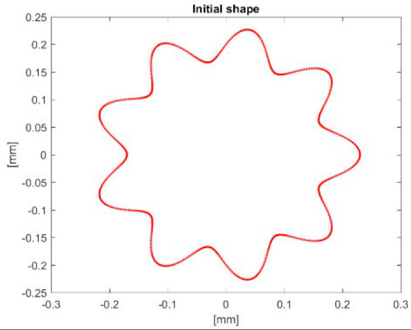
</td><td>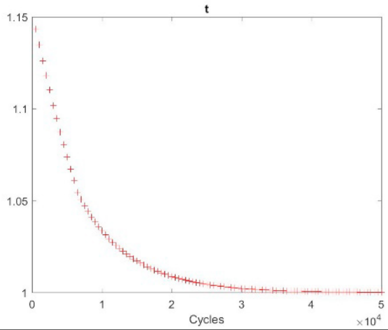
</td></tr>
<tr><td>3</td><td>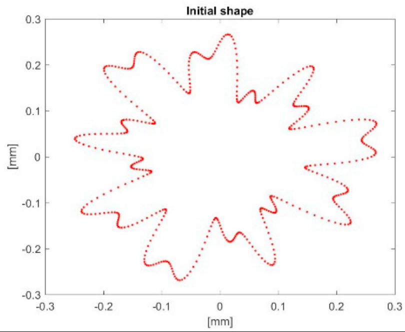
</td><td>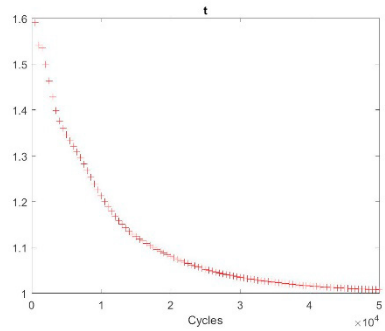
</td></tr>
<tr><td>4</td><td>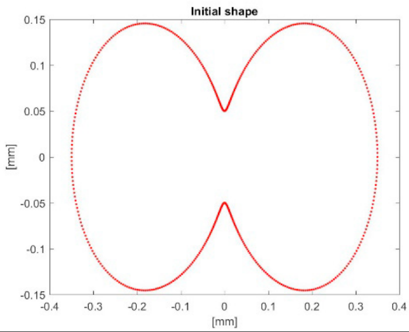
</td><td>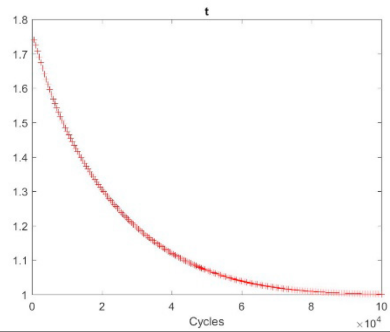
</td></tr>
</table>

4. Conclusion

In this paper, a simple model to study the crack growth of embedded three-dimensional planar cracks has been proposed. In the limit of first order approximation of the stress intensity factor and Paris-Erdogan crack propagation laws, all numerical analyses show that the flaw tends to reach a circular shape when a remote uniform fatigue stress field is imposed and the characteristic values of welded joints is used for fatigue crack propagation. In order to confirm this trend other examples are in progress.

References

[1] Tada, H., Paris, C.P., Irwin, G.R., (2000). The stress analysis of cracks handbook. Third edition, ASME press.
[2] Fett T, Munz D. Stress Intensity Factors and Weight Functions. Southampton, Computational Mechanics Publications, 1997
[3] Shah R.C., Kobayashi A.S., Stress Intensity Factors for an elliptical crack under arbitrary normal loading, Engineering Fracture Mechanics, 1971, 3, 71-96
[4] Irwin, G.R., (1962). The crack-extension force for a part-through crack in a plate. ASME, Journal of Applied Mechanics, 651-654
[5] Oore M., Burns D.J., (1980). Estimation of stress intensity factors for embedded irregular cracks subjected to arbitrary normal stress fields. Journal of Pressure Vessel Technology ASME, 102, 202-211
[6] Livieri P., Segala F., New weight functions and second order approximation of the Oore-Burns integral for elliptical cracks subject to arbitrary normal stress field. *Engineering Fracture Mechanics,* 2015, 138, pp. 100-117
[7] A. Carpinteri, R. Brighenti, S. Vantadori. Surface cracks in notched round bars under cyclic tension and bending. International Journal of Fatigue Volume 28, Issue 3, 2006, Pages 251-260
[8] BS 7608-2:1993. Fatigue design and assessment of steel structures
[9] Zerbs U T, Schödel M, Webster S, Ainsworth R 2007 Fitness-for-Service Fracture Assessment of Structures Containing Cracks: *A Workbook based on the European SINTAP/FITNET procedure*, Elsevier, 1st ed. Oxford, Amsterdam, the Netherlands
[10] Gurney, TR. (1991). *The fatigue strength of transverse fillet welded joints*. Abington Publishing, Cambridge.
[11] Carpinteri A. Shape change of surface cracks in round bars under cyclic axial loading. International Journal of Fatigue, 15 (1) 1993, 21-26
[12] Murakami Y., M. Endo (1983). Quantitative evaluation of fatigue strength of metals containing various small defects or cracks. Engineering Fracture Mechanics, 17 (1), 1-15
[13] Murakami Y., Nemat-Nasser S. (1983). Growth and stability of interacting surface Flaws of arbitrary shape Engineering Fracture Mechanics, 17 (3), 193-210
[14] Livieri P., Segala F. (2010). An analysis of three-dimensional planar embedded cracks subjected to uniform tensile stress, Engineering Fracture Mechanics, Volume 77, 2010, Pages 1656-1664
[15] Livieri P., Segala S. (2016) Stress intensity factors for embedded elliptical cracks in cylindrical and spherical vessels. Theoretical and Applied Fracture Mechanics 86(1):260–266
[16] Livieri P., Segala F. (2018) An approximation in closed form for the integral of Oore–Burns for cracks similar to a star domain. Fatigue Fract Eng Mater Struct, 41:3–19
[17] Livieri P., Segala F, Asymptotic behaviour of the Oore-Burns integral for cracks with a corner and correction formulae for embedded convex defects Engineering Fracture Mechanics 252 (2021) 107663
[18] Livieri, P. Segala, F. (2010). First order Oore–Burns integral for nearly circular cracks under uniform tensile loading. International Journal of Solids and Structures. 47(9), pp. 1167–1176
[19] Paris P, Erdogan F. A critical analysis of crack propagation laws. J Basic Eng 1963; 85:528–33
[20] Kujawski D. A new (ΔK+Kmax) 0.5 driving force parameter for crack growth in aluminum alloys. Int J Fatigue 2001; 23:733–40.
[21] Wolf E. Fatigue crack closure under cyclic tension. Eng Fract Mech 1970;2:37–45.
[22] Huang X, Moan T. Improved modeling of the effect of R-ratio on crack growth rate. Int J Fatigue 2007;29:591–602
[23] Hobbacher, AF, 2016 Recommendations for fatigue design of welded joints and components. Second edition, IIW document IIW-2259-15
[24] E. Javaheri, K. Hemmesi, P. Tempel, M. Farajian, Fatigue assessment of the welded joints containing process relevant imperfections, 2019, Welding in the World, https://doi.org/10.1007/s40194-018-00676-y
[25] C. Shao, H. Cui, F. Lu, Z. Li Quantitative relationship between weld defect characteristic and fatigue crack initiation life for high-cycle fatigue property, International Journal of Fatigue, 2019 123, 238-247
[26] Fomin F., Kashaev N., Influence of Porosity on the High Cycle Fatigue Behaviour of Laser Beam Welded Ti-6Al-4V Butt Joints. 3rd International Symposium on Fatigue Design and Material Defects, FDMD 2017, 19-22, September 2017, Lecco, Italy, Structural Integrity Procedia 7 (2017) 415–422
[27] Murakami Y. Metal Fatigue: Effects of Small Defects and Nonmetallic Inclusions. 1sted. Oxford: Elsevier; 2002. 369 p.
[28] F. Fomin, V. Ventzke, F. Dorn, N. Levichev, N. Kashaev. Effect of Microstructure Transformations on Fatigue Properties of Laser Beam Welded Ti-6Al-4V Butt Joints Subjected to Postweld Heat Treatment, DOI: 10.5772/66178
[29] Lazarus V. Brittle fracture and fatigue propagation paths of 3D plane cracks under uniform remote tensile loading. International Journal of

Fracture 2003, 122: 23–46,
[30] Bower, A. F. and Ortiz, M. (1990). Solution of Three-Dimensional Crack Problems by a Finite Perturbation Method. Journal of the Mechanics and Physics of Solids **38**(4), 443–480